

**Structural characterisation and photophysical properties of lanthanoid complexes of a tetra-amide functionalised calix[4]arene**

Christopher R. Driscoll,<sup>a</sup> Brian W. Skelton,<sup>b</sup> Massimiliano Massi,<sup>a</sup> and Mark I. Ogden<sup>a</sup>

*a. Department of Chemistry and Nanochemistry Research Institute, Curtin University, Perth, Australia*

Department of Chemistry

Curtin University

GPO Box U 1987

Perth 6845

AUSTRALIA

email: [m.ogden@curtin.edu.au](mailto:m.ogden@curtin.edu.au)

*b. Centre for Microscopy, Characterisation and Analysis, The University of Western Australia, Crawley, Western Australia 6009, Australia*

## **Structural characterisation and photophysical properties of lanthanoid complexes of a tetra-amide functionalised calix[4]arene**

Lanthanoid complexes of a tetra-amide substituted calix[4]arene in the cone conformation are characterised by single crystal X-ray structure determination. The structural analysis shows that the metal ions are coordinated to the calixarene through the eight O donor atoms, along with one aqua ligand which is located within the cavity of the calixarene. The calixarene ligand was covalently incorporated into a polymethylmethacrylate monolith through *p*-allyl functional groups, followed by loading with a range of lanthanoid cations giving rise to light-emitting materials. The emission from the hydrid materials was found to be comparable to the solution phase emission.

Keywords: calixarene; amide; lanthanide; crystal structure

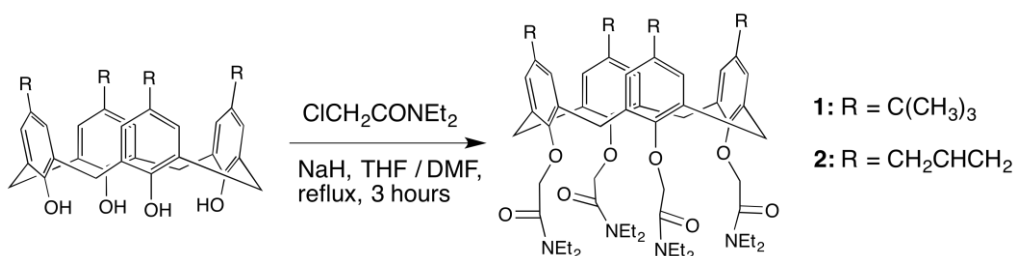
## Introduction

The synthesis and structural characterisation of the tetra-amide functionalised calix[4]arene **1**, with the crystal structure of a potassium complex, was first reported in 1987.<sup>(1)</sup> This is one of the archetypal ionophores based on the calixarene framework, and while initial studies focussed on binding of alkali metals, it was not long until studies of lanthanoid complexes of this,<sup>(2)</sup> and related,<sup>(3, 4)</sup> ionophores were reported. Investigation of the photophysics in these systems has predominantly involved complexes of europium and terbium, with modification required to achieve efficient sensitisation, particularly for europium.<sup>(4, 5)</sup> While early photophysical analysis suggested that one solvent water molecule was bound to the lanthanoid ion in complexes of **1**,<sup>(2)</sup> it is notable that no lanthanoid complex of a calix[4]arene tetraamide in the cone conformation has been structurally characterised to date in support of these solution phase studies. Structurally characterised complexes of **1** have been reported with many other metals, including Group 1<sup>(1, 6-9)</sup> and 2<sup>(8, 10, 11)</sup> cations, as well as a range of 3d element cations,<sup>(12)</sup> and main group elements such as lead<sup>(12)</sup>. In addition, metal complexes of **1** in the partial cone conformation (with lanthanum<sup>(13)</sup>), and in the 1,3-alternate conformation (with potassium<sup>(14)</sup>) have been structurally characterised. Building on our recent work with a tris-amide substituted calix[4]arene lanthanoid receptor and its incorporation into polymeric hybrid materials,<sup>(15, 16)</sup> we have synthesised the *p*-allylcalix[4]arene tetraamide **2**. While crystallisation of a lanthanoid complex of **1** continues to elude us, we report here the crystal structure determination of two lanthanoid complexes of **2**, together with the incorporation of **2** into polymeric materials to form lanthanoid-containing hybrid materials.

## Results and discussion

### *Ligand synthesis and characterisation*

Tetra-amide substituted calixarenes **1** and **2** were synthesised in the cone conformation by reaction of the parent calixarene with sodium hydride in the presence of excess 2-chloro-N,N-diethylacetamide (Scheme 1), based on the literature method.<sup>(6)</sup> Both calixarenes were synthesised in greater than 80% yield. Isolating **2** free of coordinated sodium cations proved challenging initially, and was ultimately achieved by precipitating the product from the reaction mixture by adding water, and washing the product thoroughly with water after isolating by filtration. Characterisation by  $^1\text{H}$  and  $^{13}\text{C}$  NMR spectroscopy and microanalysis, as well as crystallographic structure determination as discussed below, confirmed that the product was the target calixarene **2**.



Scheme 1. Synthesis of tetra-amide substituted calixarenes **1** and **2**.

### *Metal complexation studies*

Attempts to crystallise lanthanoid complexes of **1** and **2** were made using a range of conditions. The only successful experiments resulted in the crystallisation of complexes of **2** with neodymium and dysprosium. These complexes were crystallised by slow evaporation of a 1:1 mixture of **2**, and the appropriate precursor Ln(NO<sub>3</sub>)(DMSO)<sub>x</sub>, dissolved in DCM : ethyl acetate : methanol, 7:3:1. Both complexes crystallised as

yellow plates that were found to be of sufficient quality for single crystal X-ray structure determination.

The results of the structure determination of the neodymium complex, Nd-2 are consistent with the formulation  $[\text{Nd}_2(\text{OH}_2)][\text{Nd}(\text{NO}_3)_5(\text{dmsO})][\text{Nd}(\text{NO}_3)_4(\text{dmsO})(\text{CH}_3\text{OH})]\cdot\text{CH}_3\text{OH}\cdot\text{H}_2\text{O}$ . The calixarene-bound Nd1 atom is nine-coordinate with the coordinating atoms being the eight calixarene **2** oxygen atoms plus a water molecule which is coordinated to the metal atom and resides within the calixarene cavity (Figure 1). The coordination sphere can be described as a slightly distorted capped square antiprism with the water molecule being the capping atom. The dihedral angles between the O(n1) planes and the planes of the phenyl rings are 67.3(1), 72.3(1), 65.6(1), 67.8(1) $^\circ$  for rings 1-4. The dihedral angles between opposite phenyl rings are 47.2(2) $^\circ$  (between rings 1 and 3) and 39.9(2) $^\circ$  (between rings 2 and 4).

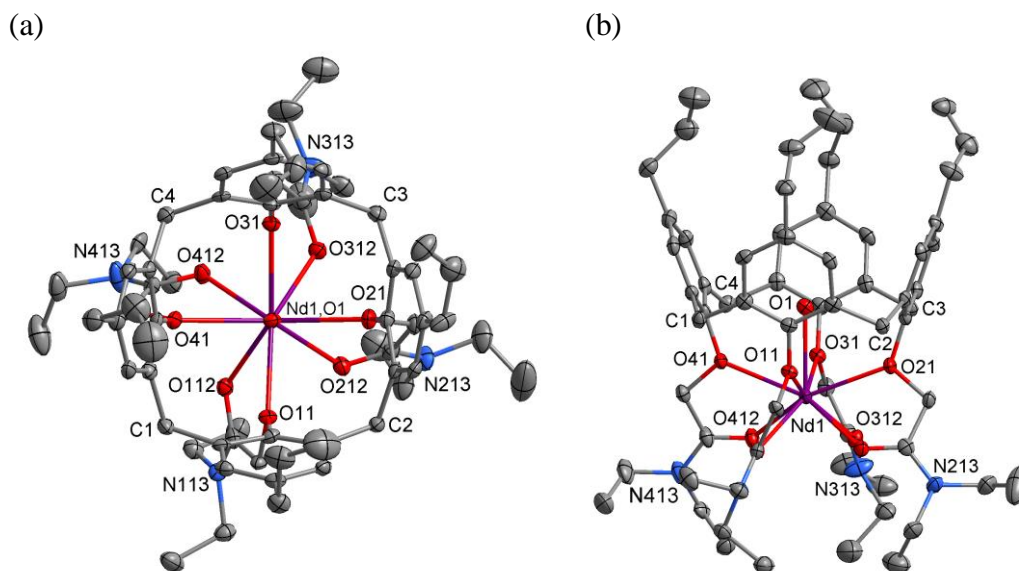


Figure 1. (a) Structure of the cation of Nd-2 projected along the pseudo 4-fold axis, (b) the cation projected oblique to (a). Hydrogen atoms and the minor component of the disordered atoms have been omitted for clarity.

Charge balance is achieved with the two complex anions  $[\text{Nd}(\text{NO}_3)_4(\text{dmsO})(\text{CH}_3\text{OH})]^-$  and  $[\text{Nd}(\text{NO}_3)_5(\text{dmsO})]^{2-}$ . All of the nitrate groups in both anions are bidentate so that the Nd(2) atom in  $[\text{Nd}(\text{NO}_3)_4(\text{dmsO})(\text{CH}_3\text{OH})]^-$  is 10 coordinate and the Nd(3) atom in  $[\text{Nd}(\text{NO}_3)_5(\text{dmsO})]^{2-}$  is 11 coordinate. A search of the CSD shows that both the  $[\text{Nd}(\text{NO}_3)_4(\text{dmsO})(\text{CH}_3\text{OH})]^-$  and  $[\text{Nd}(\text{NO}_3)_5(\text{dmsO})]^{2-}$  species appears to be previously unknown, although similar species such as  $[\text{Nd}(\text{NO}_3)(\text{CH}_3\text{OH})_2]^-$  (17) and  $[\text{Nd}(\text{NO}_3)_5(\text{OH}_2)]^{2-}$  (18, 19) have been reported. The solvent water molecule and the hydroxyl hydrogen atom of the methanol molecule coordinate to Nd(2), form hydrogen bonds to nitrate oxygen atoms thereby linking the two anions. Hydrogen bonding geometrical details are listed in Table S1 (see supplementary information).

The solvent methanol molecule is situated in the calix. Although the OH hydrogen atom was not located, there is a hydrogen bond from one of the hydrogen atoms of the coordinated water molecule to the methanol oxygen atom (see Table S1). Metal complexes of calix[4]arenes incorporating additional ligands within the cavity are known, (20, 21) but appear to be relatively rare where the calixarene has been functionalised at the phenolic rim with ligating groups. Relevant examples are the cadmium complexes of lower rim ketone and ester functionalised calix[4]arenes, where acetonitrile acts as an N-donor ligand situated within the calix cavity. (22) A lithium complex of a calix[4]arene amide has also been reported with a coordinated benzonitrile within the cavity, but here the calixarene does not act as an octadentate ligand. (23)

The structure of the complex cation in Dy-2 was found to be very similar to that observed for the neodymium complex, but with a somewhat different overall formulation of  $[\text{Dy}_2(\text{OH}_2)][\text{Dy}(\text{NO}_3)_5(\text{dmsO})](\text{NO}_3) \cdot 0.5\text{CH}_3\text{OH} \cdot 0.5\text{C}_4\text{H}_8\text{O}_2$ . The calixarene-bound Dy1 atom is again nine-coordinate with the coordinating atoms being

the eight calixarene O atoms and the water molecule O atom situated within the calixarene cavity. The dihedral angles between the O(n1) planes and the planes of the phenyl rings are 65.2(1), 70.1(1), 68.6(1), 63.6(1)° for rings 1-4. The dihedral angles between opposite phenyl rings are 46.1(2)° (between rings 1 and 3) and 46.3(1)° (between rings 2 and 4). The more symmetrical cone conformation in this structure compared to Nd-2 is presumably related to the fact that the cavity is not occupied by a methanol solvent molecule, but instead is occupied by a somewhat bulkier p-allyl functional group from a neighbouring complex cation related by an inversion centre. This results in a dimeric inclusion structure (Figure 2).

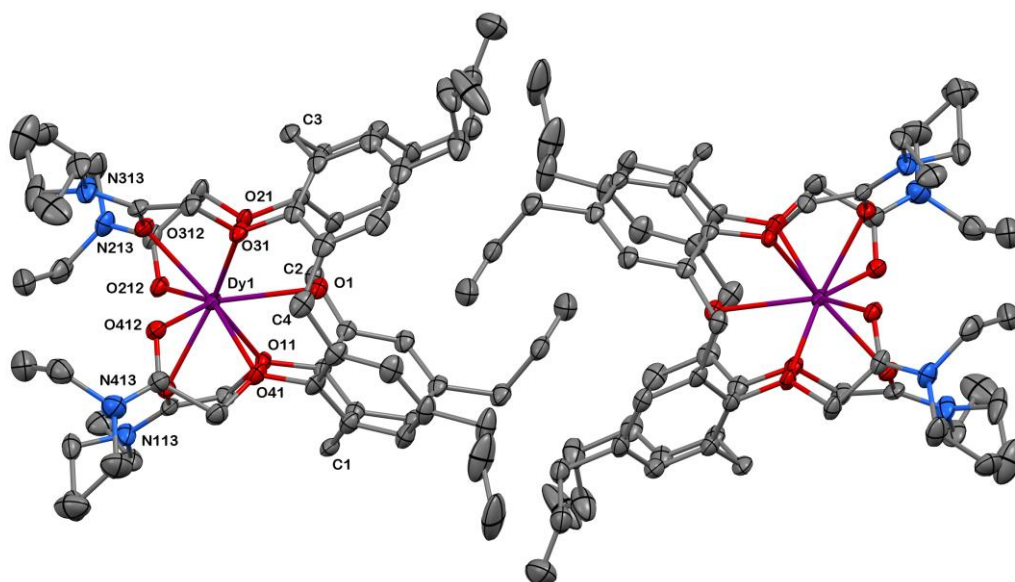


Figure 2. Structure of the cation of Dy-2, showing the inclusion of allyl groups within the cavity, leading to a supramolecular dimeric structure. The two molecules are related by an inversion centre. Hydrogen atoms and the minor component of the disordered atoms have been omitted for clarity.

Charge balance in Dy-2 is achieved with a  $[\text{Dy}(\text{NO}_3)_5(\text{dms})]^{2-}$  anion and a nitrate anion. One nitrate ligand on the complex anion  $[\text{Dy}(\text{NO}_3)_5(\text{dms})]^{2-}$  was found to be disordered over two sets of sites such that in the major component (site occupancy =

0.620(4)) it is monodentate (Dy(2)-O(501,502) 2.408(6), 3.598(6) Å) but bidentate in the minor component (site occupancy 1-0.620(4), Dy(2')-O(503,505) = 2.445(11), 2.441(11) Å). Of the other nitrate groups, three are bidentate and one is monodentate. Hence, the metal atom is 10 coordinate when the disordered nitrate is bidentate and 9 coordinate when it is monodentate. This complex anion has not been previously reported, but an analogous anion  $[\text{Dy}(\text{NO}_3)_5(\text{OH}_2)]^{2-}$  is known.(24)

A key observation from these structural studies is that the coordination of a water molecule to the lanthanoid cation bound by the calixarene is consistent with the conclusions drawn from the previously reported solution-phase photophysical studies.(2)

### ***Photophysical Characterisation***

Solutions for spectroscopic studies were prepared by adding 2 mL of a  $2 \times 10^{-5}$  M stock solution of calixarene **2** in acetonitrile to 1 mL of a  $4 \times 10^{-5}$  M stock solution of  $\text{Ln}(\text{NO}_3)(\text{DMSO})_x$  in acetonitrile. Solutions were allowed to equilibrate for 1 hour before photophysical measurements were taken.

The UV-vis absorption spectrum of calixarene **2** in acetonitrile presents a slightly structured band in the 260 to 300 nm region with  $\lambda_{\text{max}}$  at 275 nm, highlighting two peak maxima at 275 and 285 nm (See Figure S1). This band can be attributed to the  $^1(\pi-\pi^*)$  transition centred on the phenyl rings of the calixarene scaffold. The UV-vis spectra for the  $\text{Gd}^{3+}$  complex exhibited the same two peak maxima at 275 and 285 nm. The  $\text{Gd}^{3+}$  complex had a slightly lower maximum molar absorptivity with  $\epsilon_{275 \text{ nm}} = 5160 \text{ M}^{-1}\text{cm}^{-1}$  versus  $\epsilon_{275 \text{ nm}} = 5700 \text{ M}^{-1}\text{cm}^{-1}$  for the free ligand.

For calixarene **2**, excitation in this range at 77 K in acetonitrile yields a strong and structured emission band with a maximum at 300 nm, tailing off into a weak band up to 550 nm (Figure S2). Complexation with gadolinium resulted in an increase in



intensity of the latter band. Complexation with gadolinium is known to enhance intersystem crossing to the triplet excited state of the ligand and therefore we attribute the new band to emission from the triplet excited state of the ligand. The 0-phonon transition from the phosphorescent emission band around 470 nm was visually estimated to lie at  $23,809\text{ cm}^{-1}$ . This energy level is greater than the lowest energy excited states of  $\text{Tb}^{3+}$  ( $^5\text{D}_4 = 20500\text{ cm}^{-1}$ ),  $\text{Sm}^{3+}$  ( $^4\text{G}_{5/2} = 17700$ ) and  $\text{Dy}^{3+}$  ( $^4\text{F}_{9/2} = 20960\text{ cm}^{-1}$ ), which suggests a good energy transfer between calixarene **2** and the lanthanides should be possible, based on previous literature ( $\Delta E (^3\text{T}^* - \text{Ln}^*) = 2500 - 3000\text{ cm}^{-1}$ ).<sup>(25)</sup>

Complexes of calixarene **2** with  $\text{Tb}^{3+}$ ,  $\text{Dy}^{3+}$  and  $\text{Sm}^{3+}$  were luminescent in acetonitrile at room temperature, showing characteristic lanthanide metal-centred line-like emission on excitation at 270 nm (Figures 3-5). Monitoring the most intense emission band for  $\text{Tb}^{3+}$  (543 nm),  $\text{Dy}^{3+}$  (570 nm) and  $\text{Sm}^{3+}$  (600 nm), complexes showed a broad excitation with two maxima at 275 and 285 nm, corresponding closely with the peaks observed in the absorption spectra (Figure S4, 6, 8). This indicates that the metal centred emission originates as a result of energy transfer from the ligand, calixarene **2**.

Excited state lifetimes decays were recorded for the  $\text{Tb}^{3+}$  ( $\lambda_{\text{ex}} = 275\text{ nm}$ ,  $\lambda_{\text{em}} = 543\text{ nm}$ ),  $\text{Sm}^{3+}$  ( $\lambda_{\text{ex}} = 275\text{ nm}$ ,  $\lambda_{\text{em}} = 600\text{ nm}$ ) and  $\text{Dy}^{3+}$  ( $\lambda_{\text{ex}} = 275\text{ nm}$ ,  $\lambda_{\text{em}} = 570\text{ nm}$ ) complexes in acetonitrile (See Table 1). The  $\text{Tb}^{3+}$ ,  $\text{Sm}^{3+}$  and  $\text{Dy}^{3+}$  complexes were satisfactorily fit with monoexponential decays, although with the  $\text{Tb}^{3+}$  complex we observe a minor short-lived component (403  $\mu\text{s}$ , <3%). This short lived component is possibly due to variations in the coordination sphere.

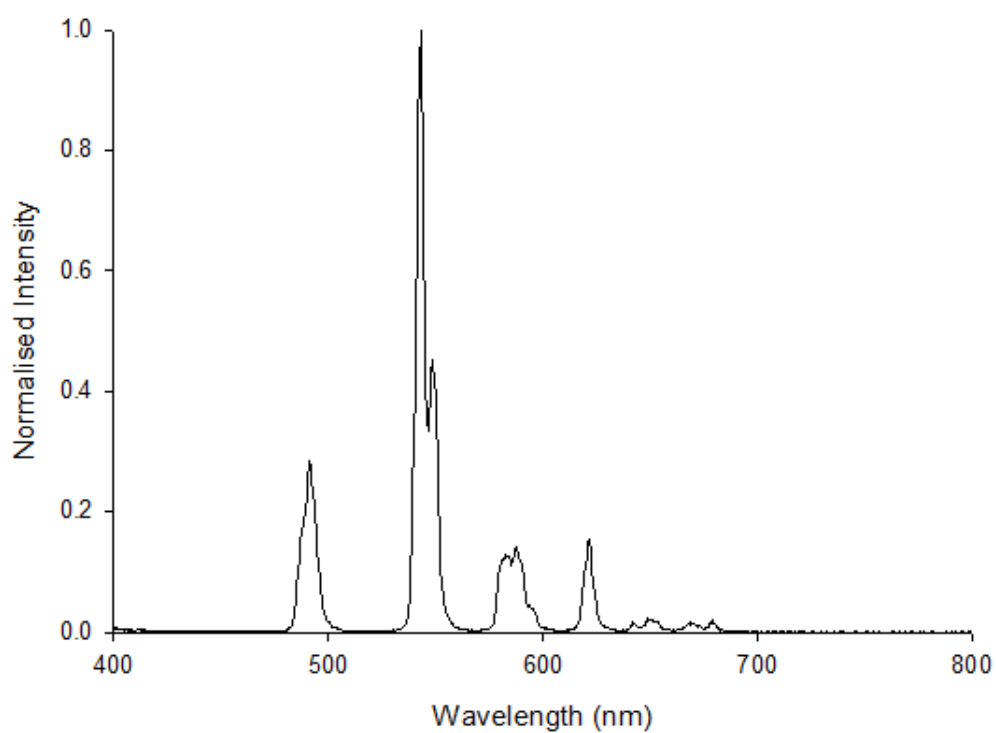


Figure 3. Emission of the calixarene **2** Tb<sup>3+</sup> complex in acetonitrile.

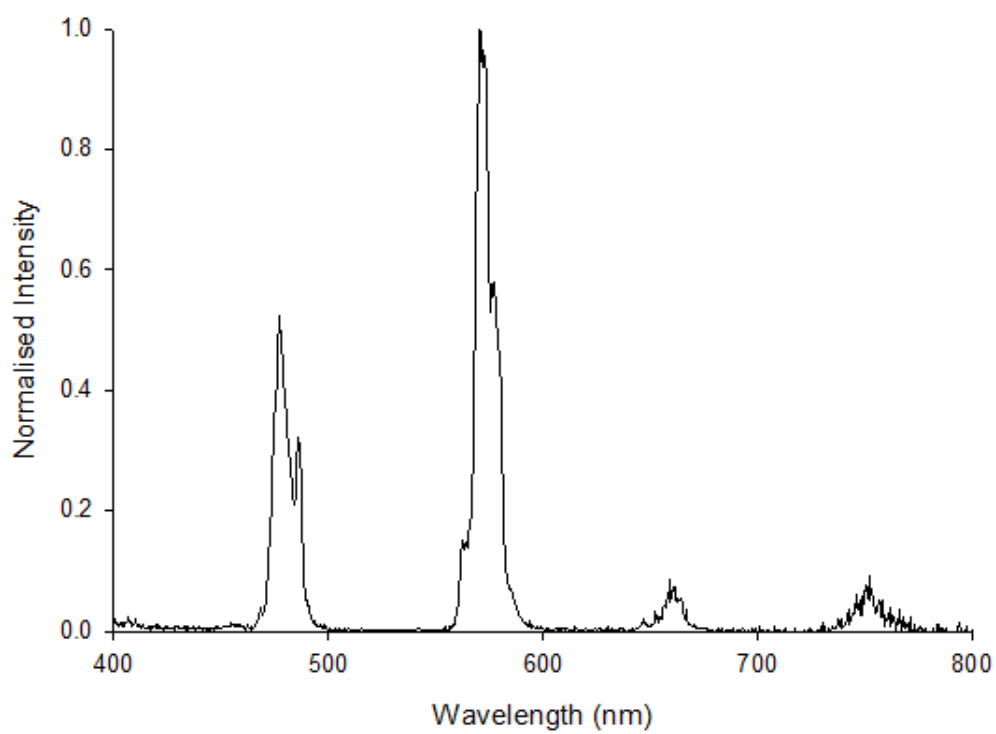


Figure 4. Emission of the calixarene **2** Dy<sup>3+</sup> complex in acetonitrile.

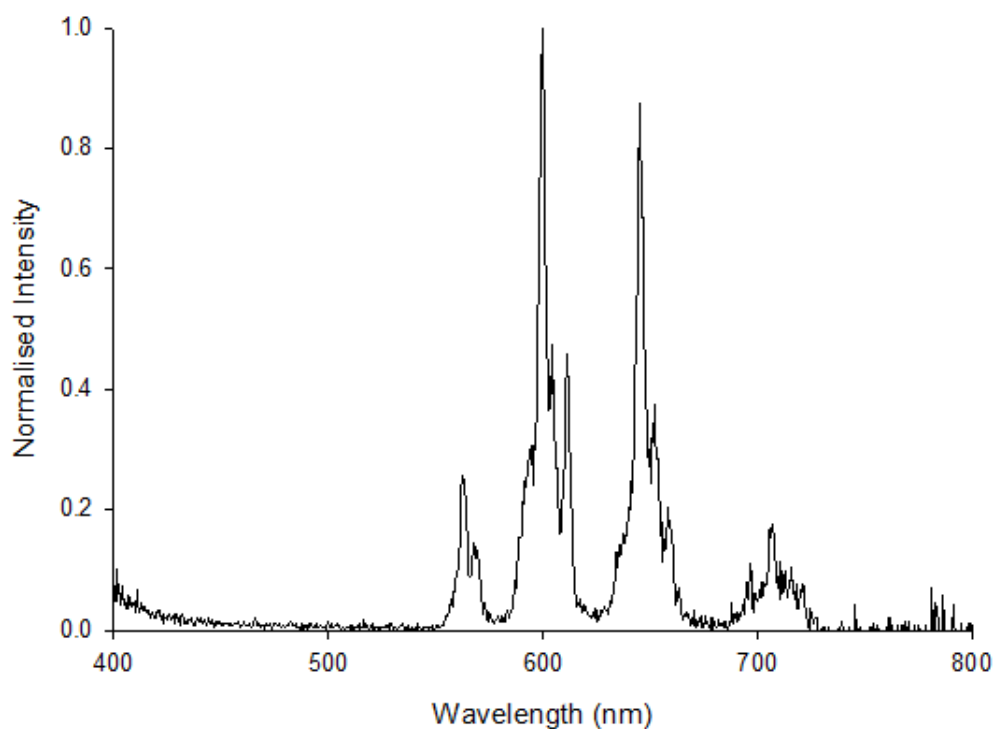


Figure 5. Emission of the calixarene **2** Sm<sup>3+</sup> complex in acetonitrile.

Table 1: Lifetimes of metal centred emission of complexes with calixarene **2** in acetonitrile.

Lanthanide	Lifetime ( $\mu\text{s}$ ) (%)
Terbium	2371
Dysprosium	30
Samarium	30

To determine the average number of coordinated OH oscillators ( $m$ ), the lifetime of the Tb<sup>3+</sup> complex was also measured in methanol ( $\tau_{\text{MeOH}} = 1707 \mu\text{s}$ ) and deuterated methanol ( $\tau_{\text{MeOD}} = 2234 \mu\text{s}$ ). Using the formula from a literature method,

$$m = a(\tau_{\text{MeOH}}^{-1} - \tau_{\text{MeOD}}^{-1}) \text{ where } \tau \text{ is in ms.}$$

$$m = 8.4(1.707^{-1} - 2.234^{-1}) = 1.16$$

where  $\tau$  is in ms and  $a$  has a value of 8.4 for  $\text{Tb}^{3+}$  in methanol,(26) it was determined that there was  $\sim 1$  molecule of methanol coordinated to the metal centre. This is also seen with the crystal structures which show water coordinated through the annulus of the calixarene **2**.

### ***Hybrid Materials***

The calixarene **2** was incorporated into PMMA monoliths as described previously for the analogous trisamide-substituted calixarene,(15, 16) using the same swelling procedure to introduce various lanthanides into the polymer matrix. When exposed to 1:1 solutions of dichloromethane:ethanol the polymer monoliths swelled in size rather than dissolving, confirming crosslinking of the polymer chains.

Polymer samples made without calixarene **2** exhibited broad, weak emission between 300 and 500 nm when excited in the 260 to 320 nm range (Figure S10). When crosslinked with calixarene **2**, several broad emission bands were observed when exciting in the same range (Figure S11). As these bands were not present in the un-crosslinked polymer it is likely they originate from the calixarene.

Emission of the  $\text{Gd}^{3+}$  containing polymer exhibited a new band compared to the blank polymer centred at 450 nm. The emission profile was much narrower than that of the  $\text{Gd}^{3+}$  complex in solution at 77K. The 0-phonon transition was visually estimated to lie at about  $23,809 \text{ cm}^{-1}$ , similar to that estimated for the solution state measurements.

Characteristic metal-centred emission was observed for  $\text{Tb}^{3+}$ ,  $\text{Sm}^{3+}$  and  $\text{Dy}^{3+}$  metal containing polymers. The excitation profile similar is to that observed for previously reported trisamide calixarene where the excitation maxima had shifted to a higher wavelength of 320nm.(15, 16) Emission from the  $\text{Tb}^{3+}$ ,  $\text{Sm}^{3+}$  and  $\text{Dy}^{3+}$  swelled

polymers when excited at 320 nm was intense compared to any residual emission from the matrix (Figures 6-9). The  $\text{Sm}^{3+}$  polymer showed some broad emission in the 400 to 500 nm range, which may be emission from the matrix.

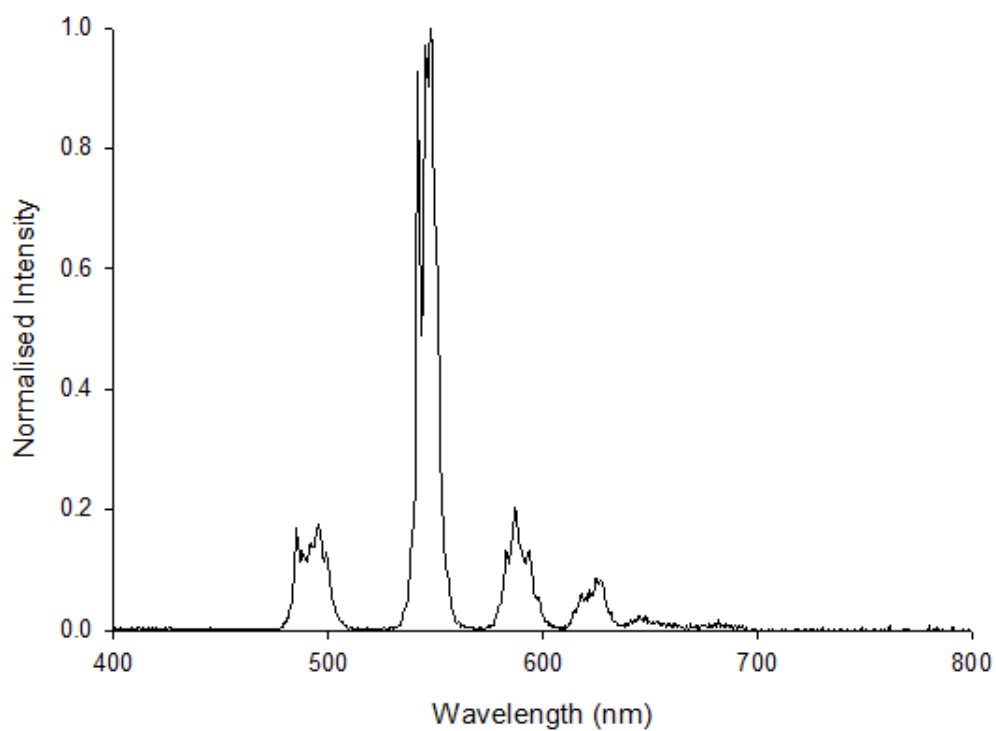


Figure 6. Emission of the polymer containing the calixarene **2**  $\text{Tb}^{3+}$  complex.

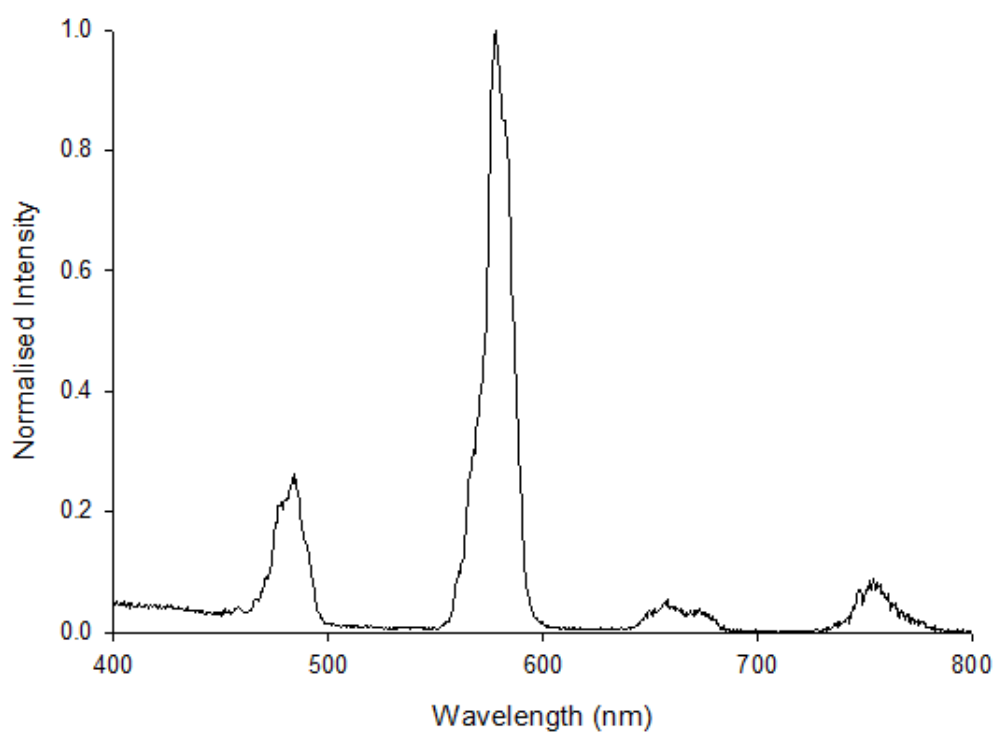


Figure 7. Emission of the polymer containing the calixarene **2** Dy<sup>3+</sup> complex.

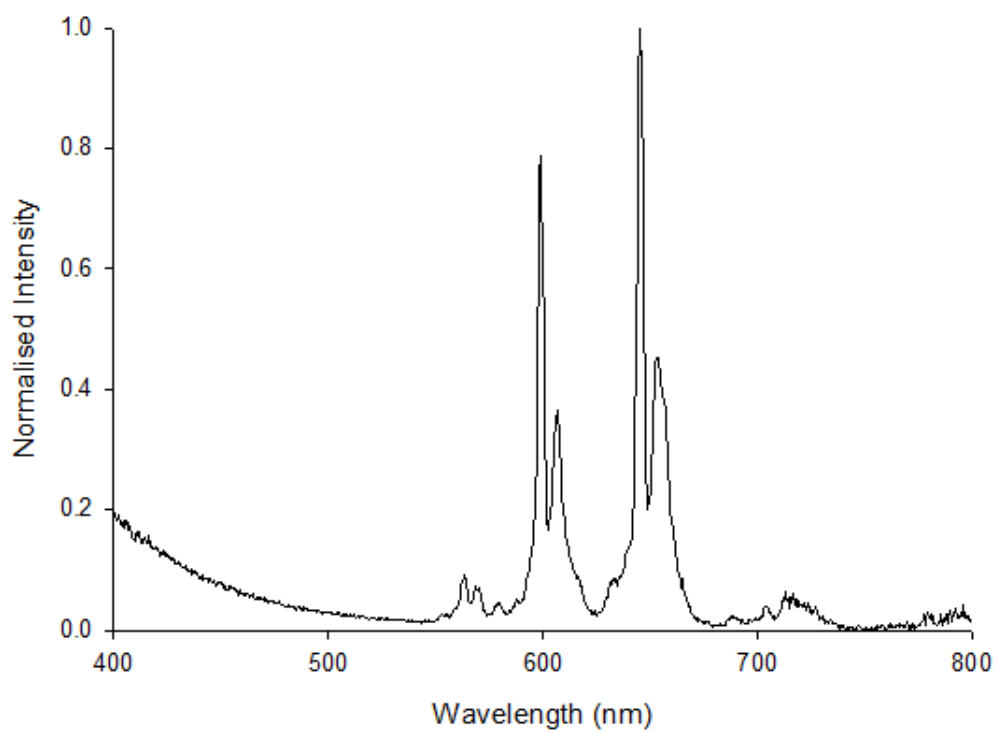


Figure 8. Emission of the polymer containing the calixarene **2** Sm<sup>3+</sup> complex.

The lifetimes of  $\text{Tb}^{3+}$  ( $\lambda_{\text{ex}} = 320 \text{ nm}$ ,  $\lambda_{\text{em}} = 543 \text{ nm}$ ) and  $\text{Dy}^{3+}$  ( $\lambda_{\text{ex}} = 320 \text{ nm}$ ,  $\lambda_{\text{em}} = 570 \text{ nm}$ ) with calixarene **2** in the polymer matrix were satisfactorily fit with multi-exponential decays (Table 2). In contrast, the  $\text{Sm}^{3+}$  containing material ( $\lambda_{\text{ex}} = 320 \text{ nm}$ ,  $\lambda_{\text{em}} = 600 \text{ nm}$ ) was best fit with a mono exponential decay. Bi-exponential nature of the lifetime of a calixarene-bound lanthanide in methylmethacrylate was also observed in previous work,<sup>(16)</sup> to which these results are comparable.

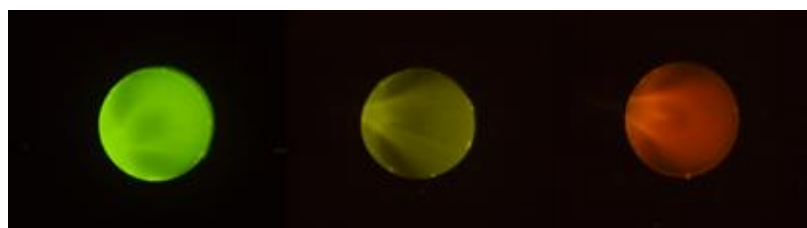


Figure 9. Visible emission from polymer monoliths of calixarene **2** containing  $\text{Tb}^{3+}$ ,  $\text{Dy}^{3+}$  and  $\text{Sm}^{3+}$  respectively.

Table 2: Lifetimes of metal centred emission in polymer monoliths.

Lanthanide	Lifetime ( $\mu\text{s}$ ) (%)
Terbium	113 (4.4), 394 (29.7) 924 (65.9)
Dysprosium	19 (83), 36 (17)
Samarium	31

## Conclusions

We have shown that lanthanoid cations bind to tetra-amide substituted calix[4]arenes through the eight O-donor atoms, along with an additional aqua ligand. The presence of a solvent molecule in the primary coordination sphere was indicated by photophysical measurements soon after this class of ionophores was first reported.<sup>(2)</sup> The work reported here confirms this and shows that, at least in the solid state, the water molecule

is situated within the calixarene cavity. Using *p*-allyl functional groups as linkers, it was shown that the calixarene ionophore could be covalently linked to a polymeric framework, and subsequently loaded with appropriate lanthanoid cations, to form light-emitting materials. The photophysical properties of the polymers were found to be similar to those observed in solution, showing that the binding site is not significantly impacted by incorporation into the polymer.

## **Experimental**

### ***General Remarks***

All reagents and solvents were purchased from chemical suppliers and used as received without further purification other than THF, which was distilled over sodium before use and methyl methacrylate which was distilled before use. Lanthanide nitrate salts were prepared by reaction of the appropriate lanthanide oxide with hot concentrated nitric acid followed by addition of minimal DMSO and precipitated with diethyl ether.

All NMR spectra were recorded using a Bruker Avance 400 spectrometer ( $^1\text{H}$  400.1 MHz,  $^{13}\text{C}$  100 MHz) at 300 K and calibrated with residual solvent signals ( $\text{CDCl}_3$   $d$   $^1\text{H}$ ,  $\delta$  7.26 ppm;  $^{13}\text{C}$ ,  $\delta$  77.16 ppm). Elemental analysis was performed by Curtin University. Melting ranges of solid samples were determined using a Barnstead/Electrothermal melting point apparatus at atmospheric pressure. Melting ranges were measured in duplicate and averaged. Photos of the polymer monolith emissions were captured by using a Nikon D300 camera with an aperture of f/9 and equipped with an OG550 EOS barrier filter.



### *General Photophysical Measurements*

UV-vis absorption spectra were obtained at room temperature using a Perkin Elmer Lambda 35 UV/Vis spectrometer. Luminescence measurements were recorded using an Edinburgh FLSO980-stm spectrometer equipped with a 450 W xenon arc lamp, double excitation and emission monochromators, and a Peltier cooled Hamamatsu R928P photomultiplier tube (185-850 nm). Emission and excitation spectra were corrected for source intensity (lamp and grating) and emission spectroscopic response (detector and grating) by a calibration curve supplied with the instrument.

Excited state decays ( $t$ ) were recorded on the same Edinburgh FLSP980-stm spectrometer using a microsecond flash-lamp with the above-mentioned R928P PMT photomultiplier as the detector. The goodness of fit was assessed by minimising the reduced  $\chi^2$  function and by visual inspection of the weighted residuals. To record the luminescence spectra at 77 K, the samples were put in quartz tubes (2 mm diameter) and inserted into a special quartz Dewar filled with liquid nitrogen. The acetonitrile solvent used in the preparation of the solutions for the photo-physical investigations were of spectrometric grade.

Photophysical properties of the polymer monoliths were measured by immobilising the monolith with the solid state stage of the fluorimeter and using a visible excitation wavelength to ensure that the polymer monolith was in the excitation beam path. All photophysical measurements of the polymers were taken at room temperature.

Calixarene free samples of polymer crosslinked with EGDMA were swelled with  $[\text{Tb}(\text{NO}_3)_3(\text{DMSO})_n]$  following the swelling procedure used for the calixarene containing polymers. This sample was excited at 320 nm and no characteristic terbium

emission was observed. Indicating that retention of the lanthanide metals in the polymers is due to the presence of the calixarene **2**.

### ***Ligand Synthesis***

*p*-Allylcalix[4]arene(27), and 5,11,17,23-tetra-*p*-*t*-butyl-25,26,27,28-tetrakis(diethylcarbamoylmethoxy)calix[4]arene **1(6)** were synthesised following literature methods.

#### *Synthesis of 5,11,17,23-Tetra-p-allyl-25,26,27,28-tetrakis(diethylcarbamoylmethoxy)calix[4]arene, 2*

*p*-Allylcalix[4]arene (1.010 g, 1.7 mmol) was added to a mixture of dry THF (40 mL)/DMF (8 mL) and stirred at room temperature for 30 minutes. The solution was then added to NaH (60% in oil, 0.611g, 15 mmol) pre-washed with hexane.  $\alpha$ -chloro-N,N-diethylacetamide (2.18 g, 12.2mmol) was then added to the mixture and stirred at 70 °C under N<sub>2</sub>. After 4 hours the reaction mixture was cooled to room temperature, most of the solvent removed *in vacuo*, and the oily residue quenched into 500 mL of water and stirred at 60-70 °C for 4 hours. This mixture was then filtered, washed with water and allowed to dry to give 1.521 g (85 % yield) of white powder. Samples for analysis were obtained by dissolving the solid in hot ethanol (10 mL) and allowing it to crystallise at -20 °C. M.p.146 -146.5 °C. <sup>1</sup>H NMR (CDCl<sub>3</sub>)  $\delta$  1.093 (12H, t, CH<sub>2</sub>-CH<sub>3</sub>), 1.156 (12H, t, CH<sub>3</sub>), 3.084 (8H, d, Ar-CH<sub>2</sub>-CH), 3.197(4H, d, Ar-CH<sub>2</sub>-Ar), 3.344(16H, m, CH<sub>2</sub>-CH<sub>3</sub>), 4.941 (8H, s, OCH<sub>2</sub>), 4.90-5.00 (8H, m, CH=CH<sub>2</sub>) 5.242 (4H, d, Ar-CH<sub>2</sub>-Ar), 5.827 (4H, m, CH=CH<sub>2</sub>), 6.498 (8H, s, Ar-H). <sup>13</sup>C NMR (CDCl<sub>3</sub>), 13.11, 14.33, 31.89, 39.37, 39.82, 40.83, 71.60, 114.74, 128.62, 133.03, 134.50, 138.38, 154.91, 168.84. Anal. Calcd for C<sub>64</sub>H<sub>84</sub>N<sub>4</sub>O<sub>8</sub>: C 74.1; H 8.16; N5.4. Found: C 73.76; H 8.37; N 5.36.

### *Crystallisation of Lanthanoid Complexes*

Calixarene **2** (0.03 g, mmol) and one equivalent of  $\text{Ln}(\text{NO}_3)(\text{DMSO})_x$  ( $\text{Ln} = \text{Nd}, \text{Dy}$ ) were dissolved in dichloromethane : ethyl acetate : methanol (7:3:1) and heated or sonicated until the solids had dissolved. The solution was then filtered through cotton wool and allowed to evaporate slowly, yielding thin, yellow plate-like crystals of Nd-**2**, or Dy-**2**.

### *Crystallography*

Crystallographic data for the structures were collected at 100(2) K on an Oxford Diffraction Gemini diffractometer fitted with Mo  $K\alpha$  radiation. Following analytical absorption corrections and solution by direct methods, the structures were refined against  $F^2$  with full-matrix least-squares using the program SHELXL-2014.(28)

Nd-**2**: One allyl and two ethyl groups were modelled as being disordered over two sets of sites with site occupancies refined to 0.621(8) and its complement for the three groups after trial refinement indicated no significant differences in the three values. The OH hydrogen atom on the methanol included within the calix was not located. The remaining hydroxyl and water molecule hydrogen atoms were located and refined with geometries restrained to ideal values. All remaining hydrogen atoms were added at calculated positions and refined by use of riding models with isotropic displacement parameters based on those of the parent atoms. Anisotropic displacement parameters were employed throughout for the non-hydrogen atoms.

Dy-**2**: The allyl groups on two of the phenyl rings were found to be disordered over two sites with site occupancies constrained to 0.5 after trial refinement. One nitrate, the dmsO and the Dy atom of the  $[\text{Dy}(\text{NO}_3)_5(\text{dmsO})]^{2-}$  anion were modelled as being

disordered over two sets of sites with occupancies refined to 0.620(4) and its complement. The geometries of the dmsu were restrained to ideal values. The solvent was modelled as a methanol molecule on general positions and an ethyl acetate molecule disordered about a crystallographic inversion centre. Both were refined with site occupancies constrained to 0.5 after trial refinement. Water molecule hydrogen atoms were located and refined with geometries restrained to ideal values. All non-solvent hydrogen atoms were added at calculated positions and refined by use of riding models with isotropic displacement parameters based on those of the parent atoms. Anisotropic displacement parameters were employed throughout for the non-hydrogen atoms.

#### *Crystal data*

Nd-2: [Nd<sub>2</sub>(OH<sub>2</sub>)] [Nd(NO<sub>3</sub>)<sub>5</sub>(dmsu)] [Nd(NO<sub>3</sub>)<sub>4</sub>(dmsu)(CH<sub>3</sub>OH)] · CH<sub>3</sub>OH · H<sub>2</sub>O

Empirical formula C<sub>70</sub>H<sub>108</sub>N<sub>13</sub>Nd<sub>3</sub>O<sub>41</sub>S<sub>2</sub>; formula weight 2284.53, monoclinic, space group *P*2<sub>1</sub>/*c*, *a* 17.0449(2), *b* 16.9624(2), *c* 31.7557(5) Å, β 91.7150(10)°, *V* 9177.2(2) Å<sup>3</sup>, *Z* 4, *D*<sub>c</sub> 1.653 Mg/m<sup>3</sup>, μ 1.814 mm<sup>-1</sup>, crystal size 0.32 x 0.11 x 0.075 mm<sup>3</sup>, θ<sub>min,max</sub> 2.10, 27.0°, reflections collected 70320, independent reflections 19878 (*R*<sub>int</sub> 0.0544), data/restraints/parameters 19878/20/1245, goodness-of-fit on *F*<sup>2</sup> 1.037, final *R* indices [*I* > 2σ(*I*)] *R*<sub>1</sub> 0.0523, *wR*<sub>2</sub> 0.1102, *R* indices (all data) *R*<sub>1</sub> 0.0742, *wR*<sub>2</sub> 0.1180. CCDC no.: 1437583.

Dy-2: [Dy<sub>2</sub>(OH<sub>2</sub>)] [Dy(NO<sub>3</sub>)<sub>5</sub>(dmsu)] (NO<sub>3</sub>) · 0.5CH<sub>3</sub>OH · 0.5C<sub>4</sub>H<sub>8</sub>O<sub>2</sub>

Empirical formula C<sub>68.50</sub>H<sub>98</sub>Dy<sub>2</sub>N<sub>10</sub>O<sub>29.50</sub>S; formula weight 1890.62, triclinic, space group *P* $\bar{1}$ , *a* 16.1254(4), *b* 16.4493(4), *c* 17.1631(4) Å, α 92.063(2), β 104.527(2)°, γ 117.004(2)°, *V* 3866.77(18) Å<sup>3</sup>, *Z* 2, *D*<sub>c</sub> 1.624 Mg/m<sup>3</sup>, μ 2.035 mm<sup>-1</sup>, crystal size 0.42

x 0.17 x 0.07 mm<sup>3</sup>,  $\theta_{\min, \max}$  2.04, 27.50°, reflections collected 44046, independent reflections 17760 ( $R_{\text{int}}$  0.0329), data/restraints/parameters 17760/104/1150, goodness-of-fit on  $F^2$  1.040, final R indices [ $I > 2\sigma(I)$ ]  $R_1$  0.0395,  $wR_2$  0.0951, R indices (all data)  $R_1$  0.0496,  $wR_2$  0.0995. CCDC no.: 1437584.

### ***Synthesis of Hybrid Materials***

Ligand 2 (0.0501 g, mmol), lauroyl peroxide (0.005g, mmol) and ethylene glycol dimethacrylate (25 uL, mmol) was dissolved in methyl methacrylate (5.3 mL, mmol). 1 mL aliquots of this solution were divided up into separate reaction containers. The reaction mixture was initiated by heating at 70 °C for 3 minutes and then quenched in an ice-water bath. Polymerisation progressed by heating at 60 °C for 2 days, then 70 °C for 24 hours. Post-polymerisation was carried out at 100 °C for 1 hour. Once separated from the reaction vessels the tubes of polymers were cut into 3-5 mm sections.

The cut sections were immersed in a 10<sup>-3</sup> M solution of the [Ln(NO<sub>3</sub>)<sub>3</sub>(DMSO)<sub>n</sub>] salts in dichloromethane-ethanol (1:1, 10 mL) for 2 days. The solution was then removed and replaced with dichloromethane-ethanol (1:1, 10 mL) for a further 2 days to remove any remaining, unbound lanthanide from the polymer matrix. This step was repeated once. The solution was then removed and the polymer monoliths allowed to de-swell at atmospheric pressure.

## Acknowledgements

We acknowledge use of the facilities and scientific and technical assistance of the Australian Microscopy and Microanalysis Research Facility at the Centre for Microscopy, Characterisation, and Analysis, The University of Western Australia, a facility funded by the University, State and Commonwealth Governments. A/Prof Simon Lewis and Jasmine McGann are kindly acknowledged for assistance with photography of the monoliths.

## References

- (1) Calestani, G.; Ugozzoli, F.; Arduini, A.; Ghidini, E.; Ungaro, R., *J. Chem. Soc., Chem. Commun.* **1987**, 344-346.
- (2) Sabbatini, N.; Guardigli, M.; Mecati, A.; Balzani, V.; Ungaro, R.; Ghidini, E.; Casnati, A.; Pochini, A., *J. Chem. Soc., Chem. Commun.* **1990**, 878-879.
- (3) Georgiev, E. M.; Clymire, J.; McPherson, G. L.; Roundhill, D. M., *Inorg. Chim. Acta* **1994**, 227, 293-296.
- (4) Steemers, F. J.; Verboom, W.; Reinhoudt, D. N.; Vandertol, E. B.; Verhoeven, J. W., *J. Am. Chem. Soc.* **1995**, 117, 9408-9414.
- (5) Lincheneau, C.; Quinlan, E.; Kitchen, J. A.; McCabe, T.; Matthews, S. E.; Gunnlaugsson, T., *Supramol. Chem.* **2013**, 25, 869-880.
- (6) Arduini, A.; Ghidini, E.; Pochini, A.; Ungaro, R.; Andreetti, G. D.; Calestani, G.; Ugozzoli, F., *J. Inclusion Phenom.* **1988**, 6, 119-134.
- (7) Wolf, N. J.; Georgiev, E. M.; Yordanov, A. T.; Whittlesey, B. R.; Koch, H. F.; Roundhill, D. M., *Polyhedron* **1999**, 18, 885-896.
- (8) Casnati, A.; Cavallo, G.; Metrangolo, P.; Resnati, G.; Ugozzoli, F.; Ungaro, R., *Chem. Eur. J.* **2009**, 15, 7903-7912.
- (9) Moser, A.; Yap, G. P. A.; Detellier, C., *J. Chem. Soc., Dalton Trans.* **2002**, 428-434.
- (10) Casnati, A.; Liantonio, R.; Metrangolo, P.; Resnati, G.; Ungaro, R.; Ugozzoli, F., *Angew. Chem. Int. Ed.* **2006**, 45, 1915-1918.
- (11) Muzet, N.; Wipff, G.; Casnati, A.; Domiano, L.; Ungaro, R.; Ugozzoli, F., *J. Chem. Soc., Perkin Trans. 2* **1996**, 1065-1075.
- (12) Beer, P. D.; Drew, M. G. B.; Leeson, P. B.; Ogden, M. I., *J. Chem. Soc., Dalton Trans.* **1995**, 1273-1283.
- (13) Beer, P. D.; Drew, M. G. B.; Ogden, M. I., *J. Chem. Soc., Dalton Trans.* **1997**, 1489-1491.
- (14) Beer, P. D.; Drew, M. G. B.; Gale, P. A.; Leeson, P. B.; Ogden, M. I., *J. Chem. Soc., Dalton Trans.* **1994**, 3479-3485.
- (15) Driscoll, C. R.; Reid, B. L.; McIldowie, M. J.; Muzzioli, S.; Nealon, G. L.; Skelton, B. W.; Stagni, S.; Brown, D. H.; Massi, M.; Ogden, M. I., *Chem. Commun.* **2011**, 47, 3876-3878.
- (16) Ennis, B. W.; Muzzioli, S.; Reid, B. L.; D'Alessio, D. M.; Stagni, S.; Brown, D. H.; Ogden, M. I.; Massi, M., *Dalton Trans.* **2013**, 42, 6894-6901.
- (17) Rajendiran, T. M.; Kahn, O.; Golhen, S.; Ouahab, L.; Honda, Z.; Katsumata, K., *Inorg. Chem.* **1998**, 37, 5693-5696.
- (18) Benetollo, F.; Bombieri, G.; Cassol, A.; Depaoli, G.; Legendziewicz, J., *Inorg. Chim. Acta* **1985**, 110, 7-13.

- (19) Yang, X. P.; Jones, R. A.; Wong, W. K.; Lynch, V.; Oye, M. M.; Holmes, A. L., *Chem. Commun.* **2006**, 1836-1838.
- (20) Taylor, S. M.; Frost, J. M.; McLellan, R.; McIntosh, R. D.; Brechin, E. K.; Dalgarno, S. J., *CrystEngComm* **2014**, *16*, 8098-8101.
- (21) Liu, L. L.; Li, H. X.; Wan, L. M.; Ren, Z. G.; Wang, H. F.; Lang, J. P., *Chem. Commun.* **2011**, *47*, 11146-11148.
- (22) de Namor, A. F. D.; Chahine, S.; Kowalska, D.; Castellano, E. E.; Piro, O. E., *J. Am. Chem. Soc.* **2002**, *124*, 12824-12836.
- (23) Horvat, G.; Stilinovic, V.; Kaitner, B.; Frkanec, L.; Tomisic, V., *Inorg. Chem.* **2013**, *52*, 12702-12712.
- (24) Nayak, S.; Novitchi, G.; Holynska, M.; Dehnen, S., *Eur. J. Inorg. Chem.* **2014**, 3065-3071.
- (25) Bünzli, J.-C.; Eliseeva, S., Basics of Lanthanide Photophysics. In *Lanthanide Luminescence*, Hänninen, P.; Härmä, H., Eds. Springer Berlin Heidelberg: 2011; Vol. 7, pp 1-45.
- (26) Holz, R. C.; Chang, C. A.; Horrocks, W. D., *Inorg. Chem.* **1991**, *30*, 3270-3275.
- (27) Gutsche, C. D.; Levine, J. A.; Sujeeth, P. K., *J. Org. Chem.* **1985**, *50*, 5802-5806.
- (28) Sheldrick, G. M., *Acta Crystallographica Section C* **2015**, *71*, 3-8.